Janus Magneto–Electric Nanosphere Dimers Exhibiting Unidirectional Visible Light Scattering and Strong Electromagnetic Field Enhancement

Hao Wang,[†,§] Pu Liu,[§] Yanlin Ke,[†,§] Yunkun Su,[†,§] Lei Zhang,[†,§] Ningsheng Xu,[†,‡,§] Shaozhi Deng,[†,‡,§] and Huanjun Chen*[,†,‡,§]

[†]State Key Laboratory of Optoelectronic Materials and Technologies, [‡]Guangdong Province Key Laboratory of Display Material and Technology, and [§]School of Physics and Engineering, Sun Yat-sen University, Guangzhou 510275, China

ABSTRACT Steering incident light into specific directions at the nanoscale is very important for future nanophotonics applications of signal transmission and detection. A prerequisite for such a purpose is the development of nanostructures with high-efficiency unidirectional light scattering properties. Here, from both theoretical and experimental sides, we conceived and demonstrated the unidirectional visible light scattering behaviors of a heterostructure, Janus dimer composed of gold and silicon nanospheres. By carefully adjusting the sizes and spacings of the two nanospheres, the Janus dimer can support both electric and magnetic dipole modes with spectral overlaps and comparable strengths. The interference of these two modes gives rise to the narrow-band unidirectional scattering behaviors with enhanced forward scattering and suppressed backward scattering. The directionality can further be improved by arranging the dimers into one-dimensional chain structures. In addition, the dimers also show remarkable electromagnetic field enhancements. These results will be important not only for applications of light emitting devices, solar cells, optical filters, and various surface enhanced spectroscopies but also for furthering our understanding on the light–matter interactions at the nanoscale.

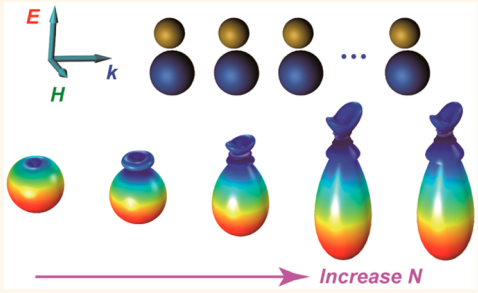

KEYWORDS: magnetic resonance · plasmon · dimer · unidirectional light scattering · electromagnetic field enhancement

During the past decades, tremendous advances have been achieved in integrated optoelectronic systems with low power consumption, fast processing speed, and highly sensitive responsivity. In order to push the envelope of these devices to meet today's explosive demands of information transfer and processing, one needs to further miniaturize various photonic structures and devices down to the nanoscale for the purpose of obtaining unprecedented operational speed and chip-scale ultracompact integration. As the sizes of the devices get smaller and approach the nanoscale, how to focus and manipulate light beyond the diffraction limit become a great challenge not only for manufacturing techniques but also for physical fundamentals. One attractive topic toward this direction is the steering of incident light into a specific direction, which is of fundamental significance for the various device applications, such as solar cells,[1] light-emitting devices,[2,3] and ultrasensitive sensors.[4,5] Conventional approaches for such purposes usually incorporate various complex architectures, such as metallic nanoantenna, photonic crystals, and metamaterials, to engineer the wavefront of the light and control its flow direction.[6−10] These structures rely on precisely locating many individual building units into specific arrangements, which usually requires very complicated and time-consuming lithography techniques and are therefore not favor for the device integration. On the other hand, localized surface plasmon resonances existing in individual metal nanostructures have expanded research in nanophotonics due to their ability to focus free-space light down to the subwavelength scale.[11−13] Under resonance excitation, the plasmonic oscillations can induce remarkable

* Address correspondence to chenhj8@mail.sysu.edu.cn.

Received for review October 1, 2014 and accepted January 2, 2015.

Published online January 02, 2015
10.1021/nn505606x

electromagnetic field enhancement in the vicinity of the nanostructures and strongly modify the localized photonic density of states, giving rise to anisotropic light radiation. However, usually only the dipolar plasmon modes can efficiently couple with the free-space optical field, and consequently, scattering patterns with doughnut shape will be obtained.[14,15] In order to direct the light scattering into one specific direction while suppressing the radiation in other unwanted directions, complex architectures with several metal nanostructures structuring into specific arrangements have to be applied.[16−18] In addition, all-metallic-type nanostructures always suffer from the high ohmic loss by the metal, which is not favorable for applications in signal generation and transmission.

In recent years, dielectric nanoparticles with a high refractive index have been shown to exhibit intriguing anisotropic light-scattering properties originated from their intrinsic optical magnetic resonances.[19−24] The presence of the magnetic modes can lead to its strong interference with the electric dipole mode of the nanoparticle, which can strongly suppress the backward scattering and lead to unidirectional forward scattering even in an individual nanoparticle.[21,25−27] However, in order to induce efficient coupling between the magnetic and electric dipole modes, the operating spectral regime should be kept within the range where the magnitudes of these two modes are equivalent to each other. Usually, such a regime is far from the resonance frequency, and therefore, the anisotropic scattering is generally weak.[28] For the sake of enhanced unidirectional scattering, one needs to generate electric and magnetic dipoles with the same resonance frequency and comparable amplitude. Recently, hybrid structures composed of dielectric and plasmonic metal components have received extensive attention due to their extraordinary optical properties derived from the synergistic interactions between these two components.[29−33] Specifically, silver core−dielectric shell nanostructures have been proposed whereby the strong coupling between the magnetic resonance of the shell the electric resonance of the core can lead to enhanced broadband forward scattering while suppressing backward scattering.[28,34−37] Although the reported results are all based on theoretical calculations, the proposed strategy has opened up a new avenue toward unidirectional light scattering.

In this paper, from both theoretical and experimental viewpoints, we present our study on realization of unidirectional forward scattering in the visible range using Janus nanosphere dimers composed of a high-refractive-index silicon nanosphere and plasmonic gold nanosphere. By properly adjusting the sizes of these two components and the spacings between them, the electric and magnetic dipoles can be tuned to have equivalent strength in a specific narrow wavelength range. In such a regime, the electric and magnetic dipole modes can interfere destructively in the backward direction but constructively in the forward direction, giving rise to unidirectional forward scattering under the excitation polarization along the dimer axis. Furthermore, the frequency regime for the unidirectional scattering can be facilely tuned by tailoring the sizes of the two nanospheres. For applications such as sensing, light-emitting devices, and photovoltaic devices, usually nanostructures with "hot-spots" of large electromagnetic field enhancement are strongly needed. We also demonstrated that remarkable electric field intensity enhancement up to 170 times can be established in the gap region between the gold and silicon nanospheres, which can further be verified using Raman spectroscopy. Finally, we showed that the directionality of the light scattering can be additionally enhanced by employing a chain of the magneto−electric Janus dimers. We want to emphasize that in prior studies metallic heterodimers with close spacing have been demonstrated to show anisotropic scattering behavior in response to different excitation directions.[37] The anisotropic scattering originates from the hybridization between various electric plasmon modes of the heterodimers due to the retardation effect, while the mechanism for unidirectional light scattering in our current study is the hybridization between electric and magnetic dipole modes with comparable magnitudes. Therefore, no phase retardation effect is needed for the anisotropic light scattering in the gold and silicon nanosphere dimers.

RESULTS AND DISCUSSION

According to the predictions using Mie theory, light scattering from spherical nanoparticles can be decomposed into a series of multipolar contributions, which is stated as[14]

$$C_{sca} = \frac{2\pi}{k^2}\sum_{n=1}^{\infty}(2n+1)(|a_n|^2+|b_n|^2) \qquad (1)$$

where k is the wavevector and a_n and b_n are the scattering coefficients standing for electric and magnetic multipolar contributions, respectively. For nanoparticles with sizes much smaller than the incident wavelength, usually only the first two terms dominate. The far-field scattering spatial distributions are determined by the interference between these different multipolar modes.[14,28] Figure 1 gives the theoretical scattering cross sections for an individual gold nanosphere and silicon nanosphere in free space, which are excited by a plane wave with linear polarization from top. The diameters of these two particles are both 150 nm. For the gold nanosphere, the scattering resonance centers at 560 nm (Figure 1a). At this resonance, the contribution from a_1 overwhelms those of the other terms, which means that the scattering in the gold nanosphere is dominated by the electric dipole mode (Figure 1a, left). As a result, the far-field scattering

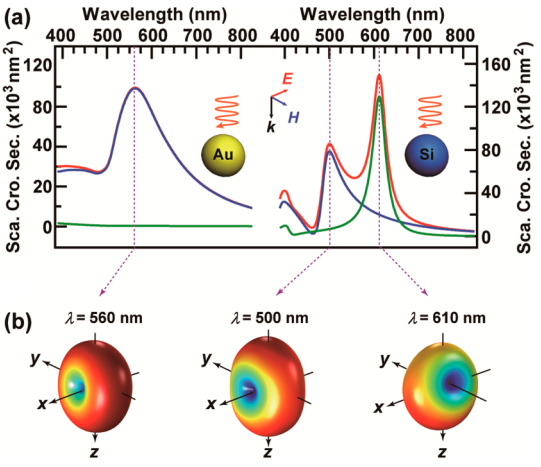

Figure 1. Calculated scattering properties of individual gold and silicon nanospheres in free space. The diameters of the gold and silicon nanospheres are both 150 nm. (a) Scattering cross sections (red) of an individual gold (left) and silicon (right) nanospheres. The contributions from the a_1 (dark blue) and b_1 (green) terms in the Mie expansion are also included. (b) Far-field scattering patterns of the three resonances: 560 nm, electric dipole mode of the gold nanosphere; 500 nm, electric dipole mode of the silicon nanosphere; and 610 nm, magnetic dipole mode of the silicon nanosphere. The nanospheres are excited by a plane wave with linear polarization from top.

exhibits a doughnut-shaped pattern with symmetric backward and forward scattering (Figure 1b). In contrast, the scattering spectrum for silicon nanosphere shows two well-defined resonance peaks (Figure 1a, right). These two peaks can be attributed to the contributions from a_1 and b_1, which are the electric (around 500 nm) and magnetic (around 610 nm) modes, respectively. Both modes are of dipolar nature with doughnut-shaped scattering patterns (Figure 1b) similar to that of the gold nanosphere. The electric and magnetic modes in the silicon nanosphere are orthogonal to each other and can interference together to suppress the backward scattering in specific frequency regime.[21,22,34] However, as mentioned above, the resulting unidirectional forward scattering by an individual silicon nanosphere is usually weak because the operating frequency is not close to both of the two resonances.

In order to obtain enhanced unidirectional scattering, one needs to create electric and magnetic dipole resonances with simultaneous spectral overlap and comparable strength. This can be understood by considering the far-field scattering intensity distribution where only the dipolar modes dominate[27,28]

$$I_{sca}(\theta, \varphi) \propto \frac{[\sin^2\varphi(a_1 + b_1\cos\theta)^2 + \cos^2\varphi(a_1\cos\theta + b_1)^2]}{k^2} \quad (2)$$

where θ and φ are the polar and azimuthal angles, respectively. For equal dipolar electric and magnetic resonances the scattering intensity is reduced to

$$I_{sca}(\theta) \propto \frac{a_1^2(1 + \cos\theta)^2}{k^2} \quad (3)$$

where the scattering is solely dependent on the polar angle between the incident and detection directions. As a result, the backward scattering ($\theta = \pi$) is completely canceled while the forward scattering ($\theta = 0$) is enhanced. Although the above analysis is based on the point dipole model, from a practical point of view, the unidirectional scattering can be realized *via* incorporation of two nanospheres with respective electric and magnetic dipole resonances. As is well-known, the electric dipole mode, or the dipolar plasmon mode, of the gold nanospheres is of surface type, making its resonance properties very sensitive to the surrounding environment. In contrast, the magnetic dipole mode supported by the silicon nanosphere is of a cavity type where the magnetic field is confined inside the nanosphere, and therefore, it is less sensitive to the surrounding environment. In this regard, one can engineer the electric and magnetic dipole resonances by placing the gold and silicon nanospheres close to each other (Figure 2a). Under excitations polarizing along the dimer axis, the electron oscillations in the gold nanosphere can strongly couple with the polarized charges within the silicon nanosphere through the Coulomb interactions. In this way, new electric and magnetic dipole modes can be formed, as will be analyzed in more detail in the following discussion. One can finely tune the strength and the frequency of these two dipole modes by carefully adjusting parameters such as the spacings of the dimer and the sizes of the nanospheres, whereby enhanced unidirectional scattering can be obtained *via* interference between the newly formed electric and magnetic dipole modes with spectral overlap.

Figure 2 gives the scattering properties of Janus dimer composed of gold and silicon nanospheres (Figure 2a) under excitation with polarization along the dimer axis from the top. The diameters of the gold and silicon nanospheres are 100 and 150 nm, respectively. When the spacing (defined as the shortest distance between the surface of the two nanospheres) between the two nanospheres is large enough (100 nm), the forward and backward scattering spectra resemble those of the individual silicon nanosphere (Figure 2b and c), with small enhanced scattering around 550 nm. This observation indicates that for large spacings the interaction between the two spheres is too weak to form strong enough new dipole modes for sufficient interferences. As a result, the scattering is dominated by the simple superposition of the contributions from both sides. As the gold nanosphere progressively approaches its dielectric counterpart, their mutual interaction becomes stronger to establish new dipole modes. When the newly formed electric and magnetic dipole modes are of comparable strengths in their spectrally overlapped regime, constructive (destructive) interference between these two modes will happen in the forward

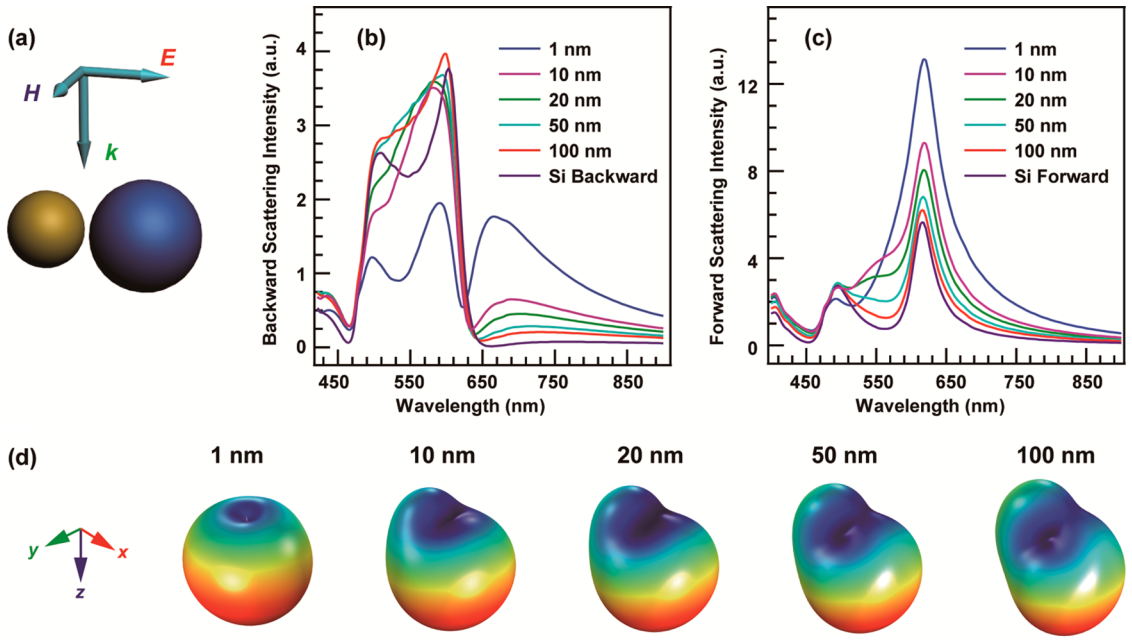

Figure 2. Calculated scattering properties of Janus dimer composed of gold and silicon nanospheres with various spacings in free space. The diameters of the gold and silicon nanospheres are 100 and 150 nm, respectively. (a) Schematic showing the Janus dimer and excitation geometry, where the dimer is excited by a plane wave polarizing along the dimer axis from top. (b) Backward scattering spectra of the Janus dimers with various spacings. (c) Forward scattering spectra of the Janus dimers with various spacings. For comparison the backward and forward scattering spectra of the individual silicon nanosphere are also included in (b) and (c). (d) Far-field scattering patterns of the Janus dimers with varying spacings.

(backward) direction, giving rise to enhanced (suppressed) forward (backward) scattering (Figure 2b,c). For example, for a dimer with spacing of 1 nm, the forward scattering intensity around the magnetic dipole mode at 620 nm is more than twice that of the individual silicon nanosphere. At the same time, the intensity for the backward scattering is only 5% of that for the forward scattering in the dimer. Such unidirectional scattering properties can be further corroborated by monitoring the dependence of the far-field scattering patterns on the spacings between the two nanoparticles at 620 nm (Figure 2d). As the gold nanosphere approaches the silicon nanosphere, the far-field scattering patterns progressively change from a doughnut-like pattern into the unidirectional forward scattering pattern with azimuthal symmetry. In addition, the unidirectional scattering is also strongly dependent on the polarization of the incident light. Pronounced unidirectional scattering only occurs using excitation polarized along the dimer axis. For excitation with polarization perpendicularly to the dimer axis, the forward and backward scattering spectra of the dimer resemble those of an individual silicon nanosphere with 150 nm diameter (Figure S1, Supporting Information). Such polarization dependence of the scattering behavior emphasizes the importance of the longitudinal (along the dimer axis) coupling of the electric and magnetic dipole modes for the unidirectional scattering.

On the basis of the above simulation results, the underlying physics of the unidirectional scattering in the Janus magneto–electric dimer structures can be further understood using the hybridization model.[12,37–40] Figure 3 illustrates how the various resonance modes in individual gold and silicon nanospheres hybridize to form the new electric and magnetic dipole modes responsible for the unidirectional scattering. The left and right panels in Figure 3a show the scattering spectra of the individual nanospheres. Together with the charge and current distributions associated with various resonances, the electric dipole mode in the gold nanosphere and the electric and magnetic dipole modes of the silicon nanosphere are clearly visible. The closeness in the energy levels of the monomers provides opportunity for the electric dipole mode (2.33 eV) of the gold nanosphere to hybridize strongly with both the electric (2.48 eV) and magnetic (2.03 eV) dipole modes of the silicon nanosphere (Figure 3b). As indicated by the dotted lines, when the dimer is formed the two electric dipole resonances will hybridize to form a new bonding electric dipole mode, which is clearly revealed in the charge distribution around the maximum (minimum) of the forward (backward) scattering. We assigned this new mode as the gap electric dipole mode (GEDM). The GEDM is a bright mode, and its line width is relatively broad. Meanwhile, because the circular electric current produced by the magnetic dipole in the silicon nanosphere is parallel to the electric dipole in the gold nanosphere, these two dipoles can also hybridize with each other to form a new resonance mode. This newly formed mode can be readily assigned as dimer magnetic mode (DMM)

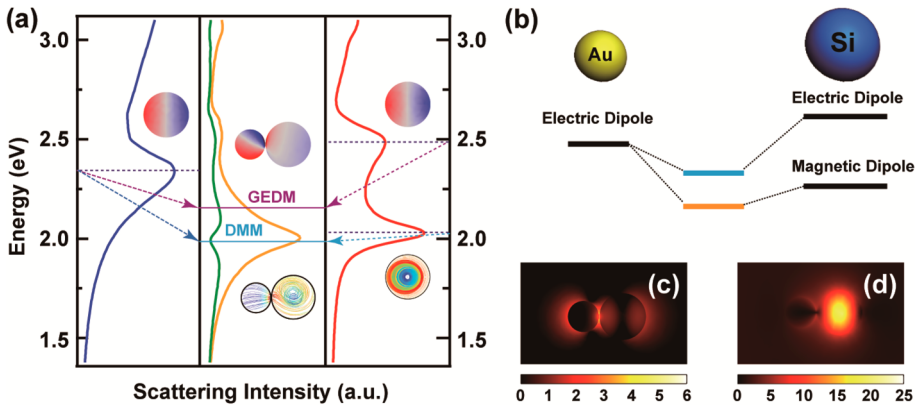

Figure 3. Hybridization model for the unidirectional scattering of the Janus dimer composed of gold and silicon nanospheres. The diameters of the gold and silicon nanospheres are 100 and 150 nm, respectively. The spacing between the two nanospheres is fixed at 1 nm. (a) Calculated scattering spectra of the individual gold nanosphere (left panel), individual silicon nanosphere (right panel), and the forward and backward scattering spectra of the Janus dimer (middle panel). Insets are the charge and current distributions corresponding to each resonance. (b) Hybridization diagram for the Janus dimer. (c) Electric field intensity enhancement contour on the central cross section of the Janus dimer. The contour is plotted at the logarithmic scale. (d) Magnetic field intensity enhancement contour on the central cross section of the Janus dimer. For (c) and (d) the dimer is excited at 620 nm with polarization along the dimer axis.

according to its related circular current distribution at the same frequency as that of the GEDM. The line width of the magnetic mode is usually narrower than that of the electric dipole mode. Therefore, the DMM is a type of dark mode. The energy level of these two modes should be different, as indicated by the energy diagram shown in Figure 3b. The "bright" GEDM and "dark" DMM have opportunity to interference with each other in a specific wavelength range where the magnitudes of these two modes are comparable with each other. Such a hybridization manner is similar to the coupling of broad bonding dipole−dipole mode and narrow bonding dipole−quadruple mode in pure metal nanosphere dimers, which leads to the Fano resonance line shape in the far-field scattering spectrum.[37] These observations unambiguously corroborate our previous standpoint that the unidirectional scattering is coming from the interference between the hybridized electric (GEDM) and magnetic (DMM) dipole modes.

Similar to the metallic and dielectric dimers, the GEDM can induce remarkable electric field intensity enhancement within the regime between the gold and silicon nanospheres.[12,41] At the forward scattering maximum the enhancement factor can be as high as 170 for dimer at the center of the gap with 1 nm width (Figure 3c). Such enhancement is larger than that induced in the pure silicon nanosphere dimers,[41] which is very promising for applications in various surface enhanced spectroscopies. On the other hand, the magnetic field enhancement at the center of the gap associated with the DMM can be up to 18 and is also larger than that of the pure silicon dimers.[41] The magnetic field enhancement is mainly confined inside the silicon nanosphere (Figure 3d), suggesting that this newly formed magnetic dipole mode is contributed mostly from that of the individual silicon nanosphere. This is reasonable because the magnetic mode of the silicon nanosphere is insensitive to the surrounding environment due to its cavity nature. By realizing this, we can further discuss one interesting behavior that in contrast to the previous study where metal core−dielectric shell nanostructures have been demonstrated to show broadband unidirectional scattering response,[28] the Janus dimer exhibits a very narrow spectral regime with distinct backward scattering suppression and forward scattering enhancement (Figure 2b and c). Such behavior can be understood *via* the hybridization model. The interference between the broad GEDM and narrow DMM can induce the narrow unidirectional scattering band. The bandwidth is mainly determined by the line width of the DMM. This interesting property can make the Janus dimers as excellent light filters and routers, which may find broad applications in future nanophotonics devices.

The above discussion suggests that the narrow wavelength regime where unidirectional scattering occurs can be tuned by tailoring the magnetic dipole mode of the silicon nanosphere. This can be done through tuning the sizes of the silicon nanospheres. Figure 4 shows the dependence of the forward/backward scattering spectra of the dimer on the sizes of the monomers. When fixing the diameter of the gold nanosphere (100 nm) while changing the sizes of the silicon nanospheres, the narrow band showing enhanced forward scattering and suppressed backward scattering strictly follows the magnetic modes of the individual silicon nanospheres (Figure 4a,b and Figure S2, Supporting Information). The backward scattering dips exhibit a nearly linear dependence on the diameters of the silicon nanospheres (Figure 4d). On the other hand, for dimers with fixed silicon nanosphere diameter (100 nm) while changing gold nanospheres,

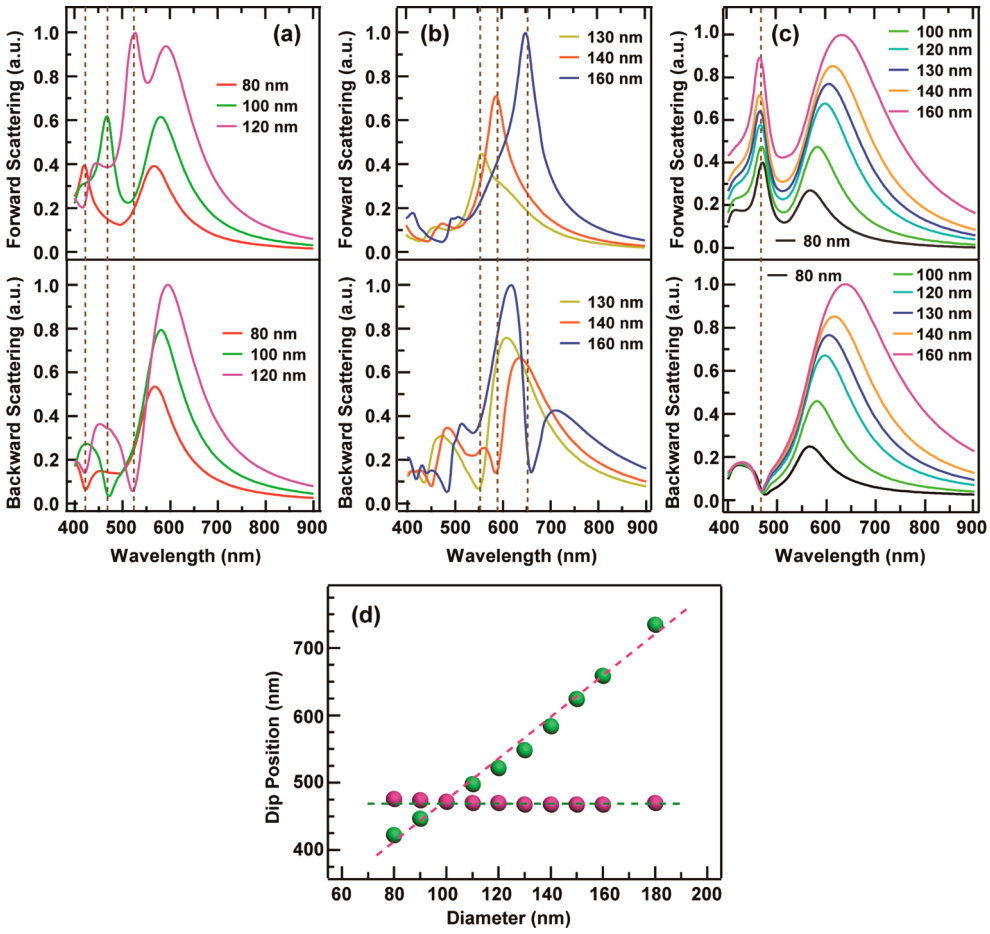

Figure 4. Dependence of the scattering properties of the Janus dimers on the diameters of the monomers in air. (a, b) Normalized forward (upper panel) and backward (lower panel) scattering spectra of dimers with varying silicon nanosphere diameters. The diameter of the gold nanosphere is fixed at 100 nm. (c) Normalized forward (upper panel) and backward (lower panel) scattering spectra of dimers with varying gold nanosphere diameters. The diameter of the silicon nanosphere is fixed at 100 nm. (d) Dependence of the dip positions with minimum backward scattering on the diameters of the gold (pink) and silicon (green) nanospheres in the dimers. The dashed lines are guides for the eyes.

the enhanced forward scattering or suppressed backward scattering band is almost invariant around the magnetic dipole resonance of the silicon nanosphere (Figure 4c,d). Moreover, by gradually increasing the diameter of the gold nanospheres, the narrow-band forward scattering can be further enhanced without deteriorating the suppressed backward scattering. All of these properties allow one to design Janus dimers to fulfill different application requirements by choosing the proper monomer sizes.

Single-particle dark-field scattering spectroscopy was then utilized to verify the unidirectional scattering properties of the Janus dimers composed of gold and silicon nanospheres. For preparation of the dimer structures, gold (NanoSeedz Ltd.) and silicon nanosphere colloidal solutions were first mixed together and 10 μL of the mixture was drop-casted onto indium tin oxide (ITO)-coated glass substrates. After the deposits were dried naturally under ambient conditions, various dimers could be formed through the joint actions of the capillary force established by the evaporating solvent and the van der Waals force between the surfactant-capped gold nanosphere and silicon nanosphere.[42] The spacings between the two nanospheres were estimated to be ~1 nm by taking into consideration the surfactant layer of the gold nanosphere.[42,43] The use of ITO substrates allows the dimers to be characterized with both scanning electron microscope (SEM) and dark-field imaging. The backward and forward scattering spectra were then measured under the dark-field microscope equipped with a spectrometer. A pattern-matching method was employed to correlate the morphology of each dimer and its scattering spectrum.[42]

We have measured various dimers with diameters of the silicon nanospheres ranging from 100 to 160 nm, while those of the gold nanospheres were fixed around 100 nm. Figure 5 shows the experimental scattering properties of three representative Janus dimers, together with their dark-field and SEM images. The scattering spectra clearly indicated that the forward (orange curves) and backward (green curves) are distinctly different from each other for every dimer (Figure 5a–c). The forward scattering overwhelms

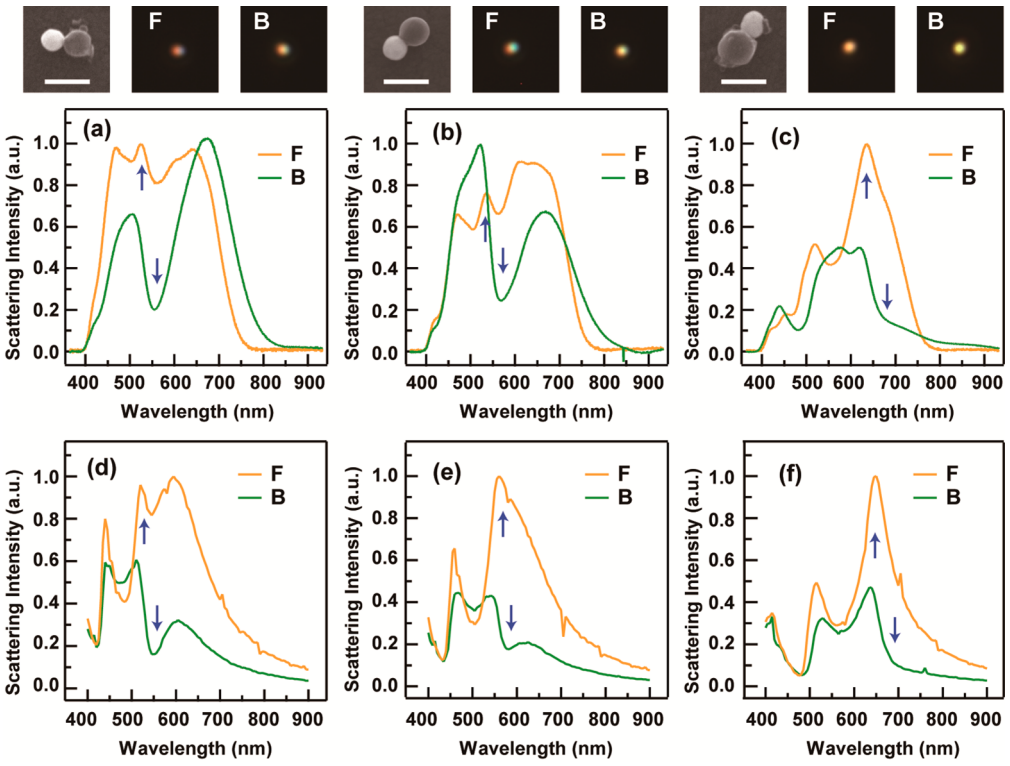

Figure 5. Experimental measurements of the scattering properties of the Janus dimers. (a−c) Forward (orange) and backward (green) scattering spectra of three typical dimers. The uppermost images are colored forward (marked with letter F) and backward (marked with letter B) dark-field scattering images and SEM images for each dimer. The scale bar in the SEM images is 200 nm. The diameters for the silicon nanospheres in the dimers are 120, 130, and 160 nm, respectively. The diameters of the gold nanosphere are fixed around 100 nm. The blue arrows indicate the maxima in the forward scattering and the sinks in the backward scattering. (d−f) The calculated forward (orange) and backward (green) scattering spectra of the three dimers shown in the SEM images. In the calculations, the dimers were supported onto ITO substrate with dielectric constant of 2.56. The specific dimer was arranged into the geometry where the axis between the centers of the gold and silicon nanospheres had an angle corresponded to the offset of their radii.

the backward scattering in broad spectral regimes. In addition, each dimer exhibits a sink on its backward scattering spectra. Corresponding to the sink position there always exists a sharp enhancement on the forward scattering spectra, as indicated by the blue arrows shown in Figure 5a−c. These anisotropic scattering behaviors are also manifested by the dark-field scattering images showing different colors in the forward and backward scattering directions for the same Janus dimer.

With the help of the dark-field spectroscopic technique, the polarization dependence of the electric and magnetic dipolar hybridization discussed above can be further corroborated using excitations with different polarizations. Although the limitation of our dark-field microscope only allows for measuring the backward scattering of the Janus dimers using excitations with polarizations parallel and perpendicular to the dimer axis (Figure S3, Supporting Information), the experimental results clearly indicate the difference between these two excitation schemes. For the three dimers we have measured, the dips in their backward scattering spectra are more pronounced under excitation polarized along the dimer axis, suggesting the importance of the longitudinal excitation for the hybridization of the electric and magnetic dipole modes.

Although the main features in the experimentally observed spectra are quite similar to those of the numerical calculations (Figure 4a,b), the deviations regarding the spectral shapes and the maxima (minima) positions are relatively large. One possible origin of such deviations is the presence of the ITO substrate in our experimental studies. The substrate will lead to redshift of the electric dipole modes, which can thereafter affect their overlaps with the magnetic mode and disturb their mutual interferences. The angular radiation pattern will also differ from that of the free-space scenario because of the dielectric interface. Furthermore, for a specific dimer supported onto the substrate, the axis between the centers of the gold and silicon nanospheres will be no longer parallel to the substrate but at an angle corresponded to the offset of their radii. This can also affect the related scattering spectra. We then performed numerical simulations by incorporation of the ITO substrate. The results clearly indicate that for a dimer composed of 100 nm gold and 150 nm silicon nanospheres these two issues only lead to small broadening of the forward

and backward scattering without modifying their overall spectral shapes (Figure S4, Supporting Information). Therefore, presence of the substrate will not strongly affect the scattering spectra of the dimers.

Another reason for the deviations refers to the excitation and collection schemes used in the experimental measurements. A previous study has shown that the collected spectra are strongly dependent on the numerical apertures of the objective used in the dark-field microscope.[44] When the forward scattering spectra of the Janus dimer were measured, the light was incident through the dark-field condenser from the bottom of the substrate (Figure S5a, yellow lines, Supporting Information). The light scattered from the dimer in the forward direction (Figure S5a, green arrows, Supporting Information) was then collected by the dark-field objective. The numerical apertures of the dark-field condenser and dark-field objective were 1.4 and 0.8, respectively. These can thereafter give incidence angles of 68° and collection angles of 53° with respect to the normal of the sample surface, respectively. Considering the light propagating along the red line, in this way the objective can simultaneously collect parts of the forward and backward scattered light. On the other hand, during backward scattering measurements, the light was shone from the upper dark-field objective (Figure S5b, yellow lines, Supporting Information). The scattered light in the backward direction (Figure S5b, blue arrows, Supporting Information) was then collected by the same objective. The geometry of the dark-field objective provided an incidence angle of ~54° with respect to the normal of the sample surface. Therefore, the collected light was also consisted of parts of forward and backward scattered light. As a result, there should be deviations between the experimental spectra and those from the simulations, which are contributed only by pure forward and backward scattered light separately.

This effect can be demonstrated by calculating the forward and backward scattering spectra of a specific Janus dimer with various incidence angles, which are defined as the angles between the incidence directions and the direction normal to the dimer axis. As the incidence angles are increased steadily while fixing the collection geometry, light scattered off to the side of incidence will be collected, instead of the pure forward/backward scattered light. Therefore, the unidirectional scattering performance of the dimer will be deteriorated (Figure S6, Supporting Information). At large enough incidence angles (>80°), the intensity of the backward scattering even overwhelms that of the forward scattering, a phenomenon opposite to our desired effect. These features has already been manifested in our experimental studies.

By realizing these features, we then calculated the scattering spectra of various Janus dimers by taking into full consideration of the experimental geometries (see the Methods for details). Two excitation polarizations, which are *s*- and *p*-polarized light, are respectively considered. For the *s*-polarized light, the polarization is parallel to the dimer axis while for the *p*-polarized light the polarization has an angle with respect to the normal of the surface. This angle is determined by the incidence angle. The total forward or backward scattering spectra are then obtained by simply summing up the contributions from these two polarization excitations. The simulation results are shown in Figure 5d–f, which indeed indicates some improvements for the agreement with the experimental measurements (Figure 5a–c). The remaining differences should be due to the nonideality of the nanosphere shapes. As already pointed out in previous study,[21] nonideality of the nanosphere shapes, as shown from the SEM images in Figure 5a–c, can strongly modify the electric and magnetic resonance wavelengths of the respective nanospheres, whereby the spectral and strength overlaps between the newly formed dipole modes will be influenced. On the other hand, due to the self-assembly process, the spacings in the dimers may more or less deviate from 1 nm utilized in the numerical calculations. Because the GEDM stems from the near-field coupling between the two nanospheres, small deviations in the spacings can lead to its strong spectral and magnitude variations, which can therefore interrupt the interference between the GEDM and DMM. One more origin for the deviations is the contamination of the nanospheres. As shown in their respective SEM images, some of the nanospheres are contaminated by several small particles or clusters, which we believe are the byproducts during the laser ablation process for fabrication of the silicon nanospheres. The presence of these contaminations can certainly alter the resonance properties of the electric and magnetic dipole modes.

As mentioned above, the hybridized GEDM can induce strong electric field enhancement inside the gap regime (Figure 3c). In order to verify this, we compared the Raman scattering spectra measured on the individual silicon nanosphere and the Janus dimer (Figure 6a). The silicon Raman signal (520 cm^{-1}) in the dimer is 2.5 times that of the individual one, justifying the existence of the strong electric field inside the gap regime. We need to mention that such Raman enhancement value is relatively low compared to typical plasmonic structures with high Raman enhancements. This is due to the relatively low electric field enhancement at the surface of the silicon nanosphere. Although at the excitation wavelength of 532 nm, the electric field enhancement at the center of the gap can be ~30 times that of an individual silicon nanosphere, the strongest enhancement at the surface of the silicon nanosphere in the dimer is only ~6. This value is only ~1.5 times that of an individual silicon

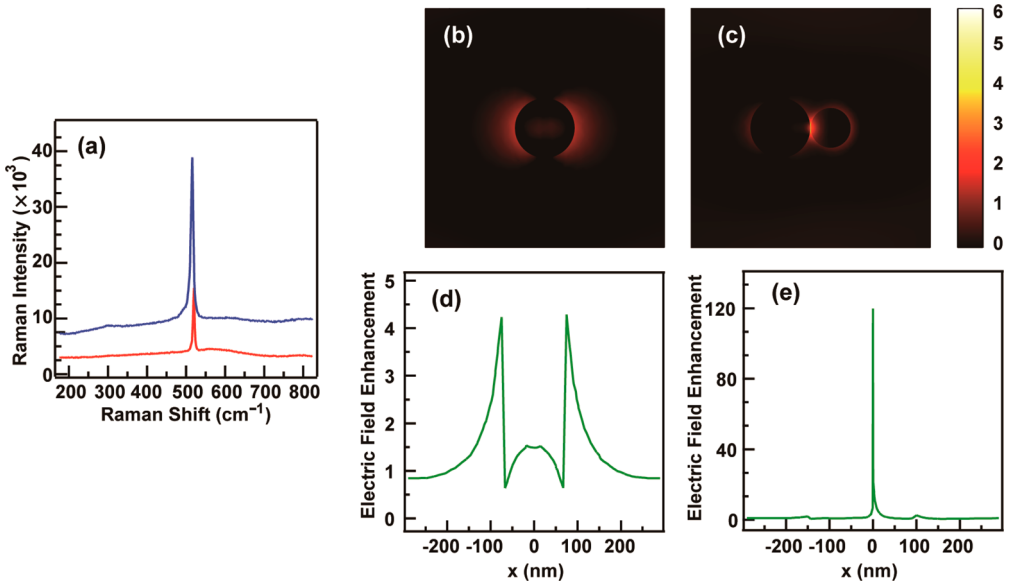

Figure 6. Enhanced Raman scattering properties of the Janus dimer. (a) Raman spectra from an individual silicon nanosphere (red) and Janus dimer (blue). The diameter of the individual silicon nanosphere is close to that in the dimer, which is ~150 nm. The diameter of the gold nanosphere in the dimer is ~100 nm. The excitation wavelength is 532 nm. (b) and (c) Calculated electric field intensity enhancement contours at 532 nm of the individual silicon nanosphere and Janus dimer at the logarithmic scale. The diameters for the silicon nanospheres in the monomer and dimer are both 150 nm. The diameter of the gold nanosphere in the dimer is 100 nm. The dimer is excited by a plane wave polarized parallel to the dimer axis from top. The individual silicon nanosphere is excited by a plane wave polarized along the diameter direction from top. (d) and (e) The related electric field enhancement distributions along the diameter of the individual silicon nanosphere and the dimer axis of the Janus dimer, respectively.

nanosphere with the same diameter (Figure 6b–e). As a result, the Raman enhancement factor from the silicon nanosphere in the dimer (approximately square of the electric field intensity) is ~6.6 compared to that of an individual silicon nanosphere, a factor close to the experimental value of 2.5. Underestimation of the enhancement factor can be also ascribed to suppression of the backward Raman scattering by the Janus dimer. Nonetheless, the strong electric field enhancement revealed in the gap regime can make the Janus dimers an excellent platform readily used in ultrasensitive sensing applications.

The unidirectional scattering from the Janus gold and silicon dimers is much different from the previous study using pure metal heterodimers.[37] In that study, the anisotropic light scattering is caused by the hybridization of different electric modes due to the retardation effect. The phase retardation can be varied using incidence light with different propagation directions. By controlling the incidence direction, a certain nanoparticle in the heterodimer can be excited more than the other, and the corresponding hybridized electric modes are then excited and give rise to a specific scattering spectrum. Without such a retardation effect, the various electric modes in the pure metal systems cannot be excited efficiently, and therefore, no anisotropic scattering can be observed. The Janus dimer proposed in this study is composed of gold and silicon nanospheres. The anisotropic light scattering is due to the hybridization of the electric and magnetic dipole modes, not pure electric modes. In this way, unidirectional forward scattering with suppressed backward scattering can be achieved once the magnitudes of the electric and magnetic dipole modes are comparable to each other. No retardation effect is needed for such anisotropic scattering, which means only light incident from one direction can lead to such unidirectional scattering. In addition, the hybridization of the electric and magnetic dipole modes in the gold and dielectric Janus dimer can give simultaneously strong electric and magnetic field enhancements in an individual dimer structure, a merit that cannot be observed in pure metal heterodimers.

The above theoretical and experimental studies unambiguously show that the Janus dimers composed of gold and silicon nanospheres with small spacings exhibit unidirectional scattering property. However, the forward scattering spatial distribution of a single dimer is still broad. In order to circumvent this problem, one-dimensional dimer chains are then utilized to improve the directionality by taking advantage of the successive backward scattering suppression and forward scattering enhancement. As shown in Figure 7a, the dimer chain is arranged with the axis parallel to the propagation direction of the incident wave, where the spacing between adjacent dimer is *d*. We then calculated the far-field scattering patterns by a chain with different dimer numbers. The spacing *d* is kept at 150 nm. The diameters of the gold and silicon nanospheres in each dimer are the same as those used in

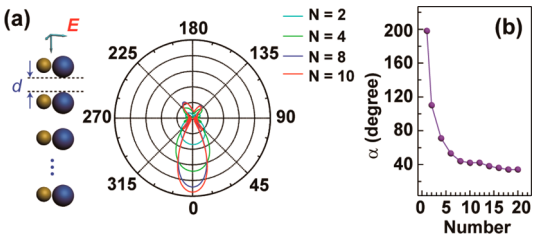

Figure 7. Unidirectional scattering properties of one-dimensional chains of Janus dimer. The chain axis is parallel to the propagation direction of the incident plane wave. The excitation polarization is along the axis of an individual dimer. (a) Scheme of the dimer chain (left) and the far-field scattering patterns of chains composed of 2, 4, 8, and 10 dimers (right). The scattering patterns are given at the principal plane defined by the incident wave vector and polarization vector. The spacings between adjacent dimers are kept at 150 nm. The polar angles are measured with origin axis pointing toward the propagating direction of the incident wave. (b) Dependence of the main lobe angular beamwidth, α, on the dimer numbers in the chain.

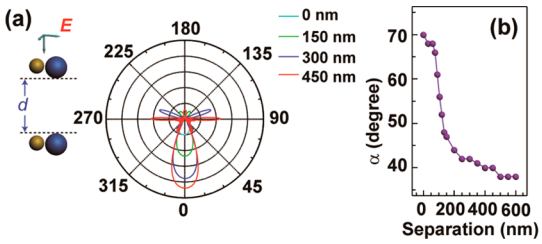

Figure 8. Dependence of the unidirectional scattering properties of the chains on the dimer spacings. The chain axis is parallel to the propagation direction of the incident plane wave. The excitation polarization is along the axis of an individual dimer. The number of dimers in the chain is fixed at 8. (a) Scheme of the dimer chain (left) and the far-field scattering patterns of chains with dimer spacings as 0, 150, 300, and 450 nm (right). The scattering patterns are given at the principal plane defined by the incident wave vector and polarization vector. The polar angles are measured with origin axis pointing toward the propagating direction of the incident wave. (b) Dependence of the main lobe angular beamwidth, α, on the dimer spacings of the chain.

Figure 2. The operating wavelength is 624 nm, which is approximately the forward scattering maximum of a single dimer. In order to characterize the directionality, we adopt the main lobe angular beamwidth, α, which corresponds to the polar angle where the scattering intensity drops to half of its maximum.[28] Figure 7a shows the far-field scattering patterns at the principal scattering plane (defined by the wave vector and polarization vector of the incident wave) by a chain with dimer numbers of 2, 4, 8, and 10. It is clearly seen that the main lobe beamwidth will decrease gradually along with increasing the number of dimers. Figure 7b indicates more clearly the dependence of α on the dimer number. By using chain composed of 20 dimers, the main lobe angular beamwidth can reduced from 200° to 34°. These behaviors unambiguously demonstrate that the unidirectional feature can be greatly enhanced using chains with large number of dimers.

On the other hand, the scattering properties of the chain are determined by the far-field interference of the many individual dimers, which relies on the phase difference between adjacent dimers. In the far-field zone, the phase difference between two adjacent dimers is $\Delta\Phi = kd(1 - \cos\theta)$,[28] indicating that the far-field scattering of the chain is strongly dependent on the spacings between adjacent dimers. The calculated scattering patterns by the chains with varying dimer spacings at 0 nm (touching dimer), 150, 300, and 450 nm are shown in Figure 8a. In the calculations, the dimer number in the chain was fixed at 8 and the operating wavelength is 624 nm. From the results, one can see clearly that the main lobe beamwidths of the chain are smaller for larger dimer spacings. By increasing the spacings to 600 nm, which is approximately the operating wavelength, the α is reduced down to 38° (Figure 8b). It is expected that the directionality can be further improved by increasing the dimer spacings. It is noted that along with increasing the dimer spacings, scattering into directions with very narrow angular distributions will occur (Figure 8a). This is a signature of the collective grating diffractions of the chain when the spacing is large enough to induce sufficient phase delay between adjacent dimers.[28] Such a grating effect will lead to energy leakage into other directions, which should be taken into account for applications such as light routing.

From an experimental point of view, stacking the Janus dimers into one-dimensional chains is very challenging. We think that this can be done *via* two approaches. The first one is the chemical assembly method. One can first functionalize the surface of the silicon nanospheres with some organic molecules. Such molecules should have the −SH group and $-OCH_3$ group (such as (3-mercaptopropyl)trimethoxysilane), whereby the gold and silicon nanospheres can be bound together to form the dimers in aqueous solution. Once the dimers have been formed, they can then be assembled into one-dimensional chains using electrostatically directed organization using polypeptide self-assembly, liquid−liquid interface assembly, pressure-driven assembly, and polymer-directed assembly approaches.[46,47] One can also use the electron beam lithography method to fabricate one-dimensional chains with stacked dimers. Such a lithography technique has already been successfully utilized for fabricating three-dimensional Yagi−Uda antennas.[48]

In comparison with the optical Yagi−Uda antennas, we think that our Janus dimer chains should have several merits. First, at the frequency where unidirectional scattering occurs, the Janus dimer chains can induce simultaneously electric and magnetic field enhancements. Second, in the dimer chain the backward scattering is suppressed automatically by each individual Janus dimer. There is no need for extra reflectors, which is pivotal element in the Yagi−Uda antenna,

to reflect the backward radiation. This can ease the fabrication complexity. Last, but not least, most of the Yagi–Uda antennas usually suffer from the high ohmic loss due to their pure metal compositions. Previous study suggested that the loss can be up to one-third of the incident energy.[49] In contrast, nearly half of the components are dielectric nanospheres in the Janus dimer chains. Therefore, the ohmic loss can be reduced remarkably, which should be more favor for applications in signal generation and transmission. In view of these findings, we believe that the Janus dimer and related one-dimensional dimer chains proposed in our study should be competitive in future nanophotonics applications of light directing and routing.

CONCLUSION

From theoretical and experimental viewpoints we have explored the unidirectional visible light scattering properties of Janus nanosphere dimers composed of gold and silicon nanospheres with small spacings. When the two nanospheres are placed close to each other, their intrinsic electric and magnetic dipole modes can hybridize to form new gap dipole modes and magnetic dipole modes. These newly formed modes can interfere with each other to give rise to the enhanced forward scattering and suppressed backward scattering. Due to the small line widths of the magnetic dipole modes, such unidirectional light scattering is of narrow-band nature. The wavelength regime where unidirectional scattering occurs can therefore be tuned by tailoring the diameters of the silicon nanospheres in the dimers. Moreover, there exists remarkable electric field enhancement within the gap regime of the Janus dimers, which can be readily used for various surface enhanced spectroscopies. We further showed that the directionality of the light scattering can be improved by arranging the dimers into one-dimensional chains with large dimer numbers and interdimer spacings. The additional interferences by the adjacent dimers can eliminate light scattering in other directions and coercively steer the incident light into the forward direction. The results found in our current study can be extended to Janus magneto–electric nanosphere dimers composed of other metal and dielectric nanospheres, which we believe will be of great interest for applications in nanoscale light focusing, manipulating, routing, and ultrasensitive biological and chemical sensings.

METHODS

Electromagnetic Numerical Simulations. Numerical simulations were performed using the commercial software package COMSOL Multiphysics v4.3b in the frequency domain. The dielectric functions of gold and silicon were employed according to previous measurements.[45] During the simulations, a linearly polarized plane wave with wavelength ranging from 430 to 900 nm was launched into a box containing the target nanostructure to simulate a propagating plane wave interacting with the nanostructure. The polarization is along the dimer axis. The nanostructure and its surrounding medium were divided using fined meshes. The surrounding medium was set as vacuum with refractive index of 1.0. Perfectly matched layers were used at the boundary to absorb the scattered radiation in all directions. The forward and backward scattering spectra were calculated by integrating the energy flow into the forward and backward hemisphere surrounding the Janus dimer. For calculating the scattering spectra of dimers supported onto the substrate, the dielectric constant of the substrate is taken as 2.56. The axis between the centers of the gold and silicon nanospheres in the dimer will be no longer parallel to the substrate but at an angle corresponded to the offset of their radii. For calculation of the backward scattering spectra, the incidence angle of the light (the *k* vector) is 54° with respect to the normal of the surface, while for calculation of the forward scattering spectra, the incidence angle of the light is 68° with respect to the normal of the surface. The collection angles for the forward and backward light scattering are both 53° with respect to the normal of the sample surface.

Synthesis of Silicon Nanospheres. In our study, the silicon nanospheres with various diameters were synthesized using the femtosecond laser ablation in liquid.[50,51] A single-crystalline silicon wafer was used as target and immersed in deionized water. A Legend Elite Series ultrafast laser (Coherent, Inc.) was utilized as the ablation source in our experiment (wavelength 800 nm). The pulse width was 35 fs, with the energy of a single pulse of 4 mJ and the repetition rate of 1 kHz. The silicon nanosphere colloidal solution could then be obtained after laser ablation of the silicon wafer in water.

Dark-Field Scattering Imaging and Spectroscopy. The scattering images and spectra of the individual Janus dimers were recorded on a dark-field optical microscope (Olympus BX51) that was integrated with a quartz tungsten halogen lamp (100 W), a monochromator (Acton SpectraPro 2360), and a charge-coupled device camera (Princeton Instruments Pixis 400BR_eXcelon). The camera was thermoelectrically cooled to −70 °C during the measurements. A dark-field objective (100×, numerical aperture 0.80) was employed for both illuminating the dimers with the white excitation light and collecting the scattered light. The scattered spectra from the individual dimers were corrected by first subtracting the background spectra taken from the adjacent regions without dimers and then dividing them with the calibrated response curve of the entire optical system. For collection of the backward scattering spectra, the light was launched from the 100× dark-field objective, and the light scattered in the backward direction was collected by the same objective. For measuring the forward scattering signal, an oil-immersed dark-field condenser with numerical aperture of 1.4 was utilized for illumination from the bottom of the sample, and the light scattering in the forward direction was recorded using the 100× dark-field objective. Color scattering images were captured using a color digital camera (ARTCAM-300MI-C, ACH Technology Co., Ltd., Shanghai) mounted on the imaging plane of the microscope. Polarization-dependent backward scattering spectra were measured according to the scheme used in previous study.[52] Briefly, a linear polarizer (U-AN360 Olympus, JAPAN) was placed in the optical path right after the white-light source. The polarization axis of the polarizer was aligned horizontally. In order to obtain a clean polarization at the substrate plane, a pinhole with a diameter of ~5 mm was inserted in the optical path right after the polarizer. The pinhole was used to select only one portion of the white light beam that was then reflected at a particular position of the circular mirror. The excitation polarization schemes were realized by rotating the sample under the dark-field objective.

Raman Spectroscopy Measurements and SEM Imaging characterizations. Raman spectra of the individual silicon nanospheres and Janus dimers were acquired using a Renishaw inVia Reflex system

equipped with a dark-field microscope (Leica). The excitation laser of 532 nm was focused onto the samples with a diameter of ~1 μm through a 50× objective (Leica, numerical aperture: 0.8). SEM imaging was performed using an FEI Quanta 450 microscope.

Conflict of Interest: The authors declare no competing financial interest.

Supporting Information Available: Calculated scattering spectra of an individual silicon nanosphere and Janus dimer composed of gold and silicon nanospheres in free space; total scattering spectra of individual silicon nanospheres with diameters of 80, 100, 120, 130, 140, and 160 nm; polarized dark-field backward scattering spectra of different Janus dimers; calculated forward and backward scattering spectra of Janus dimer supported on ITO substrate; schematic showing the forward and backward dark-field scattering spectroscopic measurements; calculated forward and backward scattering spectra of Janus dimer with various incidence angles. This material is available free of charge *via* the Internet at http://pubs.acs.org.

Acknowledgment. We thank Professor Juncong She from the School of Physics and Engineering at Sun Yat-sen University for helpful discussions. We also thank Professor Dangyuan Lei from the Department of Applied Physics at Hong Kong Polytechnic University for valuable discussions on the numerical simulations. This work was supported by the National Natural Science Foundation of China (Grant Nos. 51202300, 11474364, 51290271), the Doctoral Fund of Ministry of Education of China (Grant No. 20120171120012), the Natural Science Foundation of Guangdong Province (Grant No. S2012040007814), and the Program for Changjiang Scholars and Innovative Research Team in University (Grant No. IRT13042).

REFERENCES AND NOTES

1. Atwater, H. A.; Polman, A. Plasmonics for Improved Photovoltaic Devices. *Nat. Mater.* **2010**, *9*, 205–213.
2. Kuo, M.-L.; Kim, Y.-S.; Hsieh, M.-L.; Lin, S.-Y. Efficient and Directed Nano-LED Emission by a Complete Elimination of Transverse-Electric Guided Modes. *Nano Lett.* **2011**, *11*, 476–481.
3. Stockman, M. I. Nanoplasmonics: The Physics behind the Applications. *Phys. Today* **2011**, *64*, 39–44.
4. Ahmed, A.; Gordon, R. Single Molecule Directivity Enhanced Raman Scattering Using Nanoantennas. *Nano Lett.* **2012**, *12*, 2625–2630.
5. Wang, D. X.; Zhu, W. Q.; Best, M. D.; Camden, J. P.; Crozier, K. B. Directional Raman Scattering from Single Molecules in the Feed Gaps of Optical Antennas. *Nano Lett.* **2013**, *13*, 2194–2198.
6. Kramper, P.; Agio, M.; Soukoulis, C. M.; Birner, A.; Müller, F.; Wehrspohn, R. B.; Gösele, U.; Sandoghdar, V. Highly Directional Emission from Photonic Crystal Waveguides of Subwavelength Width. *Phys. Rev. Lett.* **2004**, *92*, 113903.
7. Curto, A. G.; Volpe, G.; Taminiau, T. H.; Kreuzer, M. P.; Quidant, R.; Van Hulst, N. F. Unidirectional Emission of a Quantum Dot Coupled to a Nanoantenna. *Science* **2010**, *329*, 930–933.
8. Lobanov, S. V.; Weiss, T.; Dregely, D.; Giessen, H.; Gippius, N. A.; Tikhodeev, S. G. Emission Properties of an Oscillating Point Dipole from a Gold Yagi–Uda Nanoantenna Array. *Phys. Rev. B* **2012**, *85*, 155137.
9. Pfeiffer, C.; Grbic, A. Metamaterial Huygens' Surfaces: Tailoring Wave Fronts with Reflectionless Sheets. *Phys. Rev. Lett.* **2013**, *110*, 197401.
10. Yu, N. F.; Capasso, F. Flat Optics with Designer Metasurfaces. *Nat. Mater.* **2014**, *13*, 139–150.
11. Schuller, J. A.; Barnard, E. S.; Cai, W. S.; Jun, Y. C.; White, J. S.; Brongersma, M. L. Plasmonics for Extreme Light Concentration and Manipulation. *Nat. Mater.* **2010**, *9*, 193–204.
12. Halas, N. J.; Lal, S.; Chang, W.-S.; Ling, S.; Nordlander, P. Plasmons in Strongly Coupled Metallic Nanostructures. *Chem. Rev.* **2011**, *111*, 3913–3961.
13. Chen, H. J.; Shao, L.; Li, Q.; Wang, J. F. Gold Nanorods and Their Plasmonic Properties. *Chem. Soc. Rev.* **2013**, *42*, 2679–2724.
14. Bohren, C. F.; Huffman, D. R. *Absorption and Scattering of Light by Small Particles*; Wiley: New York, 1983; pp 134.
15. King, N. S.; Li, Y.; Ayala-Orozco, C.; Brannan, T.; Nordlander, P.; Halas, N. J. Angle- and Spectral-Dependent Light Scattering from Plasmonic Nanocups. *ACS Nano* **2011**, *5*, 7254–7262.
16. Munárriz, J.; Malyshev, A. V.; Malyshev, V. A.; Knoester, J. Optical Nanoantennas with Tunable Radiation Patterns. *Nano Lett.* **2013**, *13*, 444–450.
17. Maksymov, I. S.; Staude, I.; Miroshnichenko, A. E.; Kivshar, Y. S. Optical Yagi–Uda Nanoantennas. *Nanophotonics* **2012**, *1*, 65–81.
18. Dorfmüller, J.; Dregely, D.; Esslinger, M.; Khunsin, W.; Vogelgesang, R.; Kern, K.; Giessen, H. Near-Field Dynamics of Optical Yagi–Uda Nanoantennas. *Nano Lett.* **2011**, *11*, 2819–2824.
19. García-Etxarri, A.; Gómez-Medina, R.; Froufe-Pêrez, L. S.; López, C.; Chantada, L.; Scheffold, F.; Aizpurua, J.; Nieto-Vesperinas, M.; Sáenz, J. J. Strong Magnetic Response of Submicron Silicon Particles in the Infrared. *Opt. Express* **2011**, *19*, 4815–4826.
20. Evlyukhin, A. B.; Novikov, S. M.; Zywietz, U.; Eriksen, R. L.; Reinhard, C.; Bozhevolnyi, S. I.; Chichkov, B. N. Demonstration of Magnetic Dipole Resonances of Dielectric Nanospheres in the Visible Region. *Nano Lett.* **2012**, *12*, 3749–3755.
21. Fu, Y. H.; Kuznetsov, A. I.; Miroshnichenko, A. E.; Yu, Y. F.; Luk'yanchuk, B. Directional Visible Light Scattering by Silicon Nanoparticles. *Nat. Commun.* **2013**, *4*, 1527.
22. Zywietz, U.; Evlyukhin, A. B.; Reinhardt, C.; Chichkov, B. N. Laser Printing of Silicon Nanoparticles with Resonant Optical Electric and Magnetic Responses. *Nat. Commun.* **2014**, *5*, 3402.
23. Kuznetsov, A. I.; Miroshnichenko, A. E.; Fu, Y. H.; Zhang, J. B.; Luk'yanchuk, B. Magnetic Light. *Sci. Rep.* **2012**, *2*, 492.
24. Coenen, T.; Van de Groep, J.; Polman, A. Resonant Modes of Single Silicon Nanocavities Excited by Electron Irradiation. *ACS Nano* **2013**, *7*, 1689–1698.
25. Gomez-Medina, R.; Garcia-Camara, B.; Suarez-Lacalle, I.; Gonzalez, F.; Moreno, F.; Nieto-Vesperinas, M.; Saenz, J. J. Electric and Magnetic Dipolar Response of Germanium Nanospheres: Interference Effects, Scattering Anisotropy, and Optical Forces. *J. Nanophotonics* **2011**, *5*, 053512.
26. Fofang, N. T.; Luk, T. S.; Okandan, M.; Nielson, G. N.; Brener, I. Substrate-Modified Scattering Properties of Silicon Nanostructures for Solar Energy Applications. *Opt. Express* **2013**, *21*, 4774–4782.
27. Person, S.; Jain, M.; Lapin, Z.; Sáenz, J. J.; Wicks, G.; Novotny, L. Demonstration of Zero Optical Backscattering from Single Nanoparticles. *Nano Lett.* **2013**, *13*, 1806–1809.
28. Liu, W.; Miroshnichenko, A. E.; Neshev, D. N.; Kivshar, Y. S. Broadband Unidirectional Scattering by Magneto–Electric Core–Shell Nanoparticles. *ACS Nano* **2012**, *6*, 5489–5497.
29. Jiang, R. B.; Li, B. X.; Fang, C. H.; Wang, J. F. Metal/Semiconductor Hybrid Nanostructures for Plasmon-Enhanced Applications. *Adv. Mater.* **2014**, *26*, 5274–5309.
30. Mongin, D.; Shaviv, E.; Maioli, P.; Crut, A.; Banin, U.; Fatti, N. D.; Vallée, F. Ultrafast Photoinduced Charge Separation in Metal–Semiconductor Nanohybrids. *ACS Nano* **2012**, *6*, 7034–7043.
31. Chen, H. J.; Shao, L.; Man, Y. C.; Zhao, C. M.; Wang, J. F.; Yang, B. C. Fano Resonance in (Gold Core)–(Dielectric Shell) Nanostructures without Symmetry Breaking. *Small* **2012**, *8*, 1503–1509.
32. Aouani, H.; Rahmani, M.; Navarro-Cía, M.; Maier, S. A. Third-Harmonic-Upconversion Enhancement from a Single Semiconductor Nanoparticle Coupled to a Plasmonic Antenna. *Nat. Nanotechnol.* **2014**, *9*, 290–294.
33. Noskov, R. E.; Krasnok, A. E.; Kivshar, Y. S. Nonlinear Metal–Dielectric Nanoantennas for Light Switching and Routing. *New J. Phys.* **2012**, *14*, 093005.
34. Liu, W.; Miroshnichenko, A. E.; Kivshar, Y. S. Control of Light Scattering by Nanoparticles with Optically-Induced Magnetic Resoponses. *Chin. Phys. B* **2014**, *23*, 047806.

35. Liu, W.; Miroshnichenko, A. E.; Oulton, R. F.; Neshev, D. N.; Hess, O.; Kivshar, Y. S. Scattering of Core−Shell Nanowires with the Interference of Electric and Magnetic Resonances. *Opt. Lett.* **2013**, *38*, 2621–2624.
36. Liu, W.; Zhang, J. F.; Lei, B.; Ma, H. T.; Xie, W. K.; Hu, H. J. Ultra-Directional Forward Scattering by Individual Core−Shell Nanoparticles. *Opt. Express* **2014**, *22*, 16178–16187.
37. Brown, L. V.; Sobhani, H.; Lassiter, J. B.; Nordlander, P.; Halas, N. J. Heterodimers: Plasmonic Properties of Mismatched Nanoparticle Pairs. *ACS Nano* **2010**, *4*, 819–832.
38. Prodan, E.; Radloff, C.; Halas, N. J.; Nordlander, P. A Hybridizaiton Model for the Plasmon Response of Complex Nanostructures. *Science* **2003**, *302*, 419–422.
39. Nordlander, P.; Oubre, C.; Prodan, E.; Li, K.; Stockman, M. I. Plasmon Hybridization in Nanoparticle Dimers. *Nano Lett.* **2004**, *4*, 899–903.
40. Davis, T. J.; Gómez, D. E.; Vernon, K. C. Simple Model for the Hybridization of Surface Plasmon Resonances in Metallic Nanoparticles. *Nano Lett.* **2010**, *10*, 2618–2625.
41. Albella, P.; Poyli, M. A.; Schmidt, M. K.; Maier, S. A.; Moreno, F.; Sáenz, J. J.; Aizpurua, J. Low-Loss Electric and Magnetic Field-Enhanced Spectroscopy with Subwavelength Silicon Dimers. *J. Phys. Chem. C* **2013**, *117*, 13573–13584.
42. Chen, H. J.; Sun, Z. H.; Ni, W. H.; Woo, K. C.; Lin, H.-Q.; Sun, L. D.; Yan, C. H.; Wang, J. F. Plasmon Coupling in Clusters Composed of Two-Dimensionally Ordered Gold Nanocubes. *Small* **2009**, *5*, 2111–2119.
43. Shao, L.; Fang, C. H.; Chen, H. J.; Man, Y. C.; Wang, J. F.; Lin, H.-Q. Distinct Plasmonic Manifestation on Gold Nanorods Induced by the Spatial Perturbation of Small Gold Nanospheres. *Nano Lett.* **2012**, *12*, 1424–1430.
44. Knight, M. W.; Fan, J.; Capasso, F.; Halas, N. J. Influence of Excitation and Collection Geometry on the Dark Field Spectra of Individual Plasmonic Nanostructures. *Opt. Express* **2010**, *18*, 2579–2587.
45. Palik, E. D. *Handbook of Optical Constants of Solids*; Academic Press: Boston, MA, 1985.
46. Guo, S. J.; Dong, S. J. Metal Nanomaterial-based self-assembly: Development, Electrochemical Sensing and SERS Applications. *J. Mater. Chem.* **2011**, *21*, 16704–16716.
47. Jeong, S.-J.; Moon, H.-S.; Shin, J.; Kim, B. H.; Shin, D. O.; Kim, J. Y.; Lee, Y.-H.; Kim, J. U.; Kim, S. O. One-Dimensional Metal Nanowire Assembly *via* Block Copolymer Soft Graphoepitaxy. *Nano Lett.* **2010**, *10*, 3500–3505.
48. Dregely, D.; Taubert, R.; Dorfmüller, J.; Vogelgesang, R.; Kern, K.; Giessen, H. 3D Optical Yagi−Uda Nanoantenna Array. *Nat. Commun.* **2011**, *2*, 267.
49. Kosako, T.; Kadoya, Y.; Hofmann, H. F. Directional Control of Light by a Nano-Optical Yagi−Uda Antenna. *Nat. Photonics* **2010**, *4*, 312–315.
50. Jiang, Y.; Liu, P.; Liang, Y.; Li, H. B.; Yang, G. W. Promoting the Yield of Nanoparticles from Laser Ablation in Liquid. *Appl. Phys. A: Mater. Sci. Process.* **2011**, *105*, 903–907.
51. Nichols, W. T.; Sasaki, T.; Koshizaki, N. Laser Ablation of a Platinum Target in Water. II. Ablation Rate and Nanoparticle Size Distributions. *J. Appl. Phys.* **2006**, *100*, 114912.
52. Chen, H. J.; Shao, L.; Ming, T.; Woo, K. C.; Man, Y. C.; Wang, J. F.; Lin, H.-Q. Observation of the Fano Resonance in Gold Nanorods Supported on High Dielectric- Constant Substrates. *ACS Nano* **2011**, *5*, 6754–6763.